AKAP350 REGULATES CYTOSKELETON REMODELLING AND LFA-1 ORGANIZATION DURING NK CYTOLYTIC RESPONSE

Alejandro P. Pariani[1], Evangelina Almada[1], Florencia Hidalgo[1], Carla Borini-Etichetti[1], Rodrigo Vena[2], Cristián Favre[1], James R. Goldenring[3], M. Cecilia Larocca[1]

[1]Instituto de Fisiología Experimental, Facultad de Ciencias Bioquímicas y Farmacéuticas, Universidad Nacional de Rosario (UNR) - Consejo de Investigaciones Científicas y Técnicas (CONICET), Rosario, Argentina; [2]Instituto de Biología Molecular y Celular de Rosario, UNR – CONICET, Rosario, Argentina; [3]Epithelial Biology Center and Department of Cell & Developmental Biology, Vanderbilt University School of Medicine, Nashville, Tennessee, USA

*Address correspondence to: M. Cecilia Larocca
Suipacha 531, 2000-Rosario, Argentina.
Phone +54-341-4305799
larocca@ifise-conicet.gov.ar

ABSTRACT

Directed secretion of cytotoxic granules into target cells constitutes a central function of natural killer (NK) cells, which requires extensive remodeling of actin and microtubule cytoskeleton at the site of NK/target cell interaction (immune synapse, IS). To date, the mechanisms coordinating cytoskeleton remodeling are not entirely understood. A-kinase anchoring protein 350 (AKAP350) is a centrosome/Golgi associated protein with a prominent role in microtubule nucleation. Our studies revealed that reduction of AKAP350 expression by stable expression of specific shRNAs inhibited actin and lymphocyte function-associated antigen-1 (LFA-1) reorganization at the IS and centrosome translocation to this site, therefore decreasing NK cytolytic activity. In NK cells, the CDC42 interacting protein 4 (CIP4) participates in centrosome translocation to the IS, where it has been proposed to integrate microtubule and actin interaction. Our studies showed that AKAP350 recruited CIP4 to the centrosome and conditioned its localization at the IS. Besides, we found that, during NK activation, AKAP350 was essential for nucleation of microtubules at the Golgi apparatus. Disruption of the Golgi function by BFA treatment or by AKAP350 delocalization from the organelle impaired LFA-1 clustering at the IS. Similarly, microtubule depolymerization and microtubule stabilization inhibited LFA-1 reorganization at the IS, without affecting actin remodeling. Altogether, our studies indicate that AKAP350 regulates distinct events at the Golgi apparatus and at the centrosome that are crucial for microtubule and actin remodelling and have a great impact on IS maturation during NK cytotoxic immune response.

INTRODUCTION

Natural killer cells (NK) are the cytolytic effectors of the innate immune system, which constitute the first line of immunological defense and are particularly relevant for the elimination of viral infected and neoplastic cells. NK cytotoxic effector function relies on the formation of a specialized junction with its target cell, generally referred to as immune synapse (IS). In the case of NK lytic IS, the persistent outside-in signaling generated by the interaction of NK activating receptors with their ligands in a susceptible target cell, in a context of absence of inhibitory signals, triggers a multistep, highly regulated process that culminates with the directed secretion of lytic molecules contained in specialized lysosomes (lytic granules) onto the target cell (Mace et al., 2014). An early event in this process is actin cytoskeleton remodeling into an F-actin-rich supramolecular activation cluster (SMAC) at the IS, and the subsequent clustering of cell-surface receptors at this site. IS maturation requires actin organization as a compact mesh at the SMAC periphery and a less dense net of branching filaments at the IS center (Brown et al., 2011), where lytic degranulation takes place (Rak et al., 2011). Immediately after actin reorganization at the IS, the centrosome, usually regarded as the main microtubule organizing center (MTOC) in NK cells, translocates to the IS, enabling lytic granules translocation and directed secretion of lytic granules contents into the target cell (Mace et al., 2014). Therefore, the development of NK lytic response requires an extensive, synchronized actin and microtubule remodeling. Even though some proteins that participate in actin and microtubule dynamics during the NK lytic IS, such as WASP (Orange et al., 2002), CDC42 (Carlin et al., 2011) and the CDC42 interacting protein 4 (CIP4) (Banerjee et al., 2007) have been identified, the mechanisms that coordinate actin and microtubule remodeling remain poorly understood.

The A-kinase anchoring protein 350 (AKAP350), also known as AKAP450, CG-NAP or AKAP9, is a centrosome and Golgi apparatus-scaffold protein (Schmidt et al, 1999) that arises as a putative candidate to regulate cytoskeleton remodeling during the development of the NK lytic response. AKAP350 has a prominent role in microtubule nucleation (Takahashi et al., 2002, Rivero et al., 2009, Kolobova et al., 2019). AKAP350 also participates in the regulation of microtubule dynamics (Larocca et., al 2006) and mitotic spindle orientation (Almada et al., 2017), and in centrosome translocation towards the leading edge in migratory cells (Tonucci et al., 2015). AKAP350 participation in microtubule remodeling is related to its capacity to scaffold specific proteins at the centrosome or at the Golgi apparatus, such as the members of the γ-TURC CGP2/3 (Takahashi et al 2002), the casein kinase δ (Sillibourne et al., 2002), CIP4 (Larocca et al., 2004), the component of the dynein/dynactin complex p150 glued (Kim et al., 2007) and the plus end binding protein 1 (EB1) (Almada el al., 2017). The involvement of AKAP350 in microtubule reorganization in response to outside-in signaling in immune cells was first revealed by studies in T cells (El Din El Homasany et al., 2005). Those studies demonstrated that the interference with AKAP350 function at the centrosome leads to inhibition of lymphocyte function-associated antigen-1 (LFA-1 or αLβ2 integrin; CD11a/CD18) induced-cell migration. Later studies indicated that, during antigen recognition by T-cells, AKAP350 participates in LFA-1 conformational activation and centrosome translocation towards the IS (Robles Valero et al., 2010). Regarding the mechanisms involved, they have not been elucidated.

In the present study we analyzed AKAP350 participation in the development of NK cytotoxic effector function and characterized its role in actin and microtubule cytoskeleton remodeling. We further characterized microtubule nucleation in activated NK cells and evaluated the role of Golgi associated AKAP350 in the IS maturation.

RESULTS

1. AKAP350 localization at the Golgi apparatus in NK/YTS cells is up-regulated during cell activation

To determine if AKAP350 could have a role in NK cytotoxic response, we first evaluated its expression in YTS immortalized NK cells. Western blot analysis of YTS cell-extracts indicates that AKAP350 is expressed in YTS cells. Immunofluorescence analysis of AKAP350 staining in resting YTS cells showed that AKAP350 colocalized with γ-tubulin and GM-130, what is indicative of AKAP350 localization at the centrosome and at the Golgi apparatus (Figure 1A, B first row). KT86 cells are susceptible targets for YTS cells, which are derived from K562 erythroleukemia cells. The analysis of YTS:KT86 conjugates indicates that AKAP350 localization at the centrosome was reduced (-50%), whereas its localization at the Golgi apparatus was increased (+44%) in activated NK cells (Figure 1A, B, second row and bars). These results indicate that activation of YTS cells induces a partial translocation of AKAP350 from the centrosome to the Golgi apparatus.

2. Decrease of endogenous AKAP350 expression impairs NK cytolytic activity

To analyze the impact of AKAP350 expression in the development of NK cytolytic effector function, we generated YTS cells with decreased AKAP350 expression (AKAP350KD) using a lentiviral short hairpin RNA expression system targeting two different AKAP350 mRNA sequences, as we have previously described (Tonucci et al., 2015). Western blot analysis of AKAP350 protein levels showed that the expression of either shRNA1 or shRNA4 efficiently decreased AKAP350 levels to less than 10% of control levels (Figure 2A). To assess AKAP350 participation in NK adhesion to target

cells, control or AKAP350KD YTS cells were labeled with TrackerTM Deep Red and KT86 cells were labeled with CFSE. Cells were incubated at different NK:target cell ratios, for different periods, and the formation of cell conjugates positive for both fluorophores was analyzed by FACS (Supplementary Figure 1). Our results showed that the decrease in AKAP350 expression did not elicit any evident effect in the initial adherence between NK and their susceptible target cells. In order to analyze NK cytolytic activity, control and AKAP350KD YTS cells generated by expression of shRNA1 or shRNA4 were incubated with CFSE-labeled KT86 cells at different NK:target cell ratios and target cell lysis was analyzed by FACS analysis of propidium iodide stained cells (Figure 2B,C). Our results showed that the decrease in AKAP350 levels by expression of either shRNA1 or shRNA4 impaired NK citolytic activity.

3. AKAP350 participates in centrosome translocation towards the lytic IS

Our previous studies demonstrated that AKAP350 regulates centrosome translocation towards the leading edge in migratory cells, a process with some homology to the development of the IS. Considering that centrosome translocation to the IS is a critical step in NK cytolytic response, centrosome localization in control and AKAP350KD YTS cells conjugated with KT86 target cells was evaluated by confocal microscopy (Figure 3A). To discriminate YTS cells from target cells, KT86 cells were preloaded with CFSE. γ-tubulin staining was used to identify the centrosome, and the IS was defined as the region of YTS/KT86 contact delimited in the DIC channel. Centrosome translocation was impaired in YTS cells with decreased expression of AKAP350, as denoted by the increased distance between the MTOC and the centroid of the IS region in AKAP350KD cells. In non cytolytic T cells, AKAP350 participates in LFA-1 activation and the subsequent translocation of the centrosome to the IS (Robles Valero et al., 2010). Considering that LFA-1 activation is sufficient to induce MTOC

translocation in NK cells, we analyzed AKAP350 role in MTOC translocation upon specific activation of LFA-1 or CD28, an additional NK receptor that induces MTOC translocation as well (Chen et al., 2006). YTS cells activated on slides coated with ICAM-1 or with an activating anti-CD28 antibody were stained and analyzed by confocal microscopy (Figure 3B,C). In both conditions, AKAP350KD cells showed an impairment in MTOC translocation towards the activating surface. Therefore, AKAP350 participates in MTOC translocation by regulating processes that are common to the activation of both LFA-1 and CD28 receptors.

4. AKAP350 regulates CIP4 localization in NK cells

CIP4 is a CDC42 effector protein involved in regulation of membrane curvature and actin remodeling. In activated NK cells, CIP4 localizes at the MTOC and at the IS and regulates MTOC translocation towards the IS (Banerjee et al., 2007). Considering that AKAP350 interacts with CIP4 and regulates its subcellular localization (Larocca et al 2004, Tonucci et al 2015), we evaluated CIP4 localization at the centrosome in control and AKAP350KD YTS cells (Figure 4A). Immunofluorescence analysis by confocal microscopy showed that CIP4 localization at the MTOC was significantly decreased in AKAP350KD YTS cells. In order to validate those results, subcellular fractions enriched in centrosomes were prepared by differential centrifugation on a Ficoll cushion, and CIP4 levels at those fractions were analyzed by western blot. Estimates considering total protein recovery and CIP4 band density at total cell lysates and at centrosomal fractions indicated that 3.0 % of total CIP4 localized at the centrosome in control cells, whereas CIP4 yield at centrosomal fraction was reduced to 1.5 % in AKAP350KD cells (Figure 4B), thus ratifying that AKAP350 participates in CIP4 recruitment to the centrosome in YTS cells. In order to analyze the relevance of AKAP350 in CIP4 localization during the development of the lytic IS, CIP4 localization

in YTS:KT86 conjugates was analyzed by confocal microscopy. Similarly to our results in resting cells, the analysis of YTS:KT86 conjugates showed that CIP4 localization at the centrosome was decreased in AKAP350KD cells (Figure 4C). Furthermore, CIP4 localization at the IS was also impaired in AKAP350KD cells (Figure 4C). By means of its amino-terminal domain CIP4 can interact with the microtubules, therefore, we further analyzed CIP4 in situ interaction with microtubules. Control and AKAP350KD cells were activated with ICAM-1 and extracts of stabilized microtubules and associated proteins were prepared. The western blot analysis of those extracts indicated that a significant fraction of CIP4 was associated with microtubules in control cells and that this fraction was significantly reduced in AKAP350KD cells (Figure 4D). It is noteworthy that α-tubulin recovery in those microtubule extracts was also diminished in AKAP350KD cells. In order to evaluate if this decrease in α-tubulin recovery in microtubule extracts was associated with decreased microtubule stability, we analyzed the relative levels of acetylated α-tubulin in NK cell lysates by western blot. Similarly to what was previously described in motile T cells (Ong et al., 2018), ihe decrease in AKAP350 expression was associated with a decrease in α-tubulin acetylation in YTS cells, thus indicating decreased microtubule stability in AKAP350KD NK cells (Supplementary Figure 2A). CIP4 yield in AKAP350KD microtubule extracts relativized to α-tubulin yield was also reduced (Figure 4D), suggesting that AKAP350 participates in CIP4 recruitment to the microtubule cytoskeleton, independently of its role in the regulation of microtubule stability.

5. The decrease in AKAP350 expression impairs actin remodeling in activated NK cells

We analyzed if actin remodeling during NK cell activation was preserved in AKAP350KD cells. Analysis YTS:KT86 conjugates by confocal microscopy indicated decreased actin accumulation at the IS in AKAP350KD cells (Figure 5A). Analysis of

YTS:KT86 conjugates morphology indicated that the surface of interaction between both cells was reduced in AKAP350KD cells, which was verified by a reduction in the IS area to 50% of control levels ($p<0.01$). The decrease in the area of effector:target cell interaction is usually associated with decreased integrin-clustering. Consistently, LFA-1 reorganization at the IS was impaired in AKAP350KD cells (Figure 5A). Similarly, inhibition of actin and LFA-1 reorganization was also observed in AKAP350KD cells when they were specifically activated with ICAM-1 or with the activating anti-CD28 antibody (Figure 5B,C). The analysis of actin distribution within the IS indicate that control YTS cells showed the characteristic actin pattern of a compact ring in the periphery with less dense actin organization at the center of the IS, whereas AKAP350KD cells showed a more homogeneous actin organization (Figure 5D). LFA-1 clustering at the periphery of the IS was also impaired in AKAP350KD cells (Figure 5D). Those results indicated that the decrease in AKAP350 expression inhibited actin remodeling and LFA-1 clustering at the IS in YTS:KT86 conjugates, thus impairing lytic IS maturation.

6. Microtubule cytoskeleton integrity is necessary for LFA-1 organization at the IS

In certain conditions, microtubule targeting drugs inhibits NK cytotoxic response (Fong et al., 2019). Nevertheless, microtubule participation in the initial events that condition the maturation of NK lytic IS has not been thoroughly evaluated. We analyzed actin remodeling at the IS in conditions where microtubule integrity was compromised, in the presence of microtubule-targeting drugs at levels that inhibit NK cytotoxicity. We found that neither cold-induced microtubule depolymerization in the presence of Nocodazole nor suppression of microtubule dynamic instability with Taxol have a significant effect on total actin accumulation at the IS (Figure 6). Regarding LFA-1 organization at the

IS, both treatments elicited similar effects, inhibiting LFA-1 accumulation and distribution at the IS (Figure 6).

7. AKAP350 participates in microtubule nucleation at the Golgi apparatus in activated NK cells

Previous studies demonstrate that AKAP350 can modulate microtubule nucleation at the Golgi apparatus and at the centrosomes in different systems (Takahashi et al, 2002; Rivero et al, 2009; Ori-McKenney et al, 2012; Maia et al, 2013; Tonucci et al, 2018). To our knowledge, microtubule nucleation at the Golgi apparatus in NK cells has not been analyzed so far. Therefore, we analyzed microtubule nucleation at the centrosome and at the Golgi apparatus in activated YTS cells, using ice recovery assays as previously described (Grimaldi et al, 2013). In conditions of YTS cell activation with ICAM-1 and anti-CD28 receptor antibody, control cells showed Golgi and centrosome nucleation of microtubules (Figure 7A, first row). AKAP350KD cells, in contrast, showed almost exclusive centrosome nucleation of microtubules (Figure 7A, second row). Quantitative analysis of newly nucleated microtubules indicated a significant reduction in Golgi associated microtubules in AKAP350KD cells (Figure 7B, upper bars), whereas no differences were observed for centrosome-associated microtubules (Figure 7B, lower bars). Similar results were obtained at 3 min (Figure 7) or 7 min (not shown) of recovery.

8. Golgi apparatus integrity is essential for the IS maturation in NK cells

As delineated above, during YTS cell activation AKAP350 translocates to the Golgi apparatus (Figure 1) where it is essential for microtubule nucleation (Figure 7). In order to analyze if AKAP350 participation in NK IS maturation could be associated with its function at the Golgi apparatus, we analyzed NK cytolytic function and IS development in cells subjected to BFA treatment. Brefeldin A inhibits the activation of ADP-

ribosylation factors, leading to the collapse of the Golgi and its redistribution into the ER (Chardin and McCormick, 1999). Previous studies showed that Brefeldin-A treatment induced relocalization of AKAP450 from the Golgi apparatus to ER exit sites and decreased MT nucleation at the Golgi apparatus (Rivero et al. 2009). Our results showed that NK cytolytic function was impaired in BFA treated cells (Figure 8A). Analysis of actin and LFA-1 distribution at the IS showed that BFA-induced impairment of YTS cytolytic function was associated with the inhibition of LFA-1 organization at the IS (Figure 8B,C), whereas actin organization was preserved (data not shown). To specifically examine the relevance of AKAP350 localization at the Golgi in the maturation of NK lytic IS, we prepared YTS cells with stable expression of AKAP350(1-1229) (AKAP350GBD) domain, which acts as a dominant negative construct that displaces the protein from the Golgi apparatus, inhibiting microtubule nucleation at this organelle (Hurtado et al 2011). Similarly to what we observed in AKAP350KD cells, relative levels of acetylated α-tubulin were decreased in AKAP350GBD cells (Supplementary figure 2B), indicating it was associated to the decreased AKAP350 expression at this organelle. Analysis of actin organization at the IS by confocal microscopy showed that actin-remodeling was preserved, whereas LFA-1 reorganization was compromised in AKAP350GBD cells (Figure 8D,E). Overall, this set of data showed that the Golgi apparatus participates in NK cytolytic response by being directly involved in LFA-1 clustering and gave strong evidence supporting a role for Golgi derived microtubules in this effect.

DISCUSSION

NK cytotoxic effector function depends on the extensive remodeling of actin and microtubule cytoskeleton, which has been extensively characterized (reviewed in

Lagrue et al, 2013). Nevertheless, the mechanisms coordinating cytoskeleton reorganization are not completely understood. In the present study, we provide evidence that AKAP350 acts as a scaffold protein that integrates events that are central for both microtubule and actin organization, therefore regulating the development of NK lytic IS. Furthermore, our results indicate that the Golgi apparatus acts as a MTOC in activated NK cells and reveals a novel role for this organelle in the maturation of the lytic IS.

In the present study, we found that normal levels of AKAP350 expression are required for MTOC translocation to the IS during the development of NK lytic response. Previous studies by Banerjee and col (2007) demonstrated that CIP4 localizes to the centrosome and to the IS in activated NK cells and that it has a central role in centrosome translocation to the IS. CIP4 is a F-BAR protein initially identified by its ability to interact with the activated form of CDC42 (Aspenström 1997). As the other members of the F-BAR family of proteins, CIP4 contains an amino-terminal domain that interacts with negatively charged membrane phospholipids promoting membrane curvature (Roberts-Galbraith and Gould, 2010). In the present work, using biochemical and immunofluorescence microscopy-assays, we found that AKAP350 is essential for CIP4 localization at the centrosome both in resting and in activated YTS cells. These results give central cues on how CIP4, a protein essentially associated with phospholipid membranes, interacts with the only non-membranous organelle in NK cells and suggest that, homologously to what was described in migratory cells, AKAP350/CIP4 protein complex could act in concert to regulate centrosome translocation towards the IS. Our data further showed that AKAP350 conditions CIP4 localization at the IS. Besides its F-BAR domains, CIP4 also contains a Src Homology 3 (SH3) domain at the carboxyl terminus that mediates its interaction with the proline-

rich domains of WASP (Tian et al, 2000). WASP is an activator of the Arp2/3 complex that promotes the formation of branched actin filaments, being positively regulated in this function by CDC42 (Leibfried et al., 2008). In NK cells, WASP colocalizes with actin at the IS, playing a central role in the development of the cytotoxic response (Orange et al., 2002). Interestingly, CDC42 activity increases at the IS very early during NK cell activation (Carlin et al, 2011). In this scenario, CIP4 could act as an adaptor that enables WASP activation by CDC42 at NK lytic IS. Moreover, by means of its SH3 domain, CIP4 also interacts with formins Dia and DAAM1 (Tsujita et al., 2006; Aspenström et al., 2006). Formins generate linear actin filaments which, in T cells, constitute the central region of the IS and are essential for integrin clustering and IS maturation (Murugesan et al., 2016). In NK cells, Dia localizes centrally at the IS and participates in targeting microtubules to this site, where lytic degranulation occurs (Butler and Cooper, 2009). Therefore, CIP4 localization at the IS could be central for the maturation of the F-actin-rich SMAC at the IS. In this regard, the decrease in CIP4 expression does not affect total actin accumulation at the IS, indicating that CIP4 does not participate in inicial actin nucleation, but it is involved in later events that are central for the maturation of the IS (Banerjee et al., 2007). How AKAP350, which specifically localizes to the Golgi apparatus and the centrosome, conditions CIP4 localization at the IS is not clear. In this regard, there is evidence supporting two putative mechanisms: 1. AKAP350 regulates CIP4 T225 phosphorylation by PKA, which controls its localization in invadopodia and its interaction with CDC42 (Tonucci et al., 2019); similarly, AKAP350 could integrate regulatory events that condition CIP4 localization at the IS. 2. CIP4 recovery in microtubule extracts was decreased in AKAP350KD cells. As we discuss below, microtubule dynamics is altered in AKAP350KD cells.

Therefore, AKAP350 could regulate CIP4 localization at the IS by enabling cellular events that condition CIP4 trafficking towards the IS.

Microtubules can regulate actin remodeling in dissimilar scenarios where polarized actin organization is required, such as integrin mediated phagocytosis (Lewkowicz et al., 2008), directional cell migration (Waterman-Storer & Salmon, 1999) and epithelial apical pole-differentiation (Mattaloni et al, 2012; Tonucci et al, 2018). Microtubule´s role in actin-organization at the IS was not clear. Microtubule targeting agents have paradoxical effects on NK cells cytotoxicity, what seems to be related to the concentration and the type of microtubule targeting agent evaluated (Katz et al., 1982; Fong et al., 2019). We found that levels of nocodazole that actually inhibits NK cytotoxicity (Katz et al., 1982), induce a defect in LFA-1 organization at the IS, but does not elicit any effect on actin organization. Orange et al have previously demonstrated that neither cell-surface receptor nor F-actin accumulation at the activating NK IS were disrupted with colchicine (Orange et al., 2003). Colchicine and nocodazole have similar mechanisms of action: both drugs bind to the β tubulin subunit blocking α/β heterodimers polymerization (Florian and Mitchison 2016). Nevertheless, in our study we additionally induced microtubule depolymerization by ice incubation, which leads to a more robust disruption of microtubule integrity. Our results also showed that micromolar levels of the microtubule stabilizing agent Taxol, which impedes microtubule growing and shortening events (Derry et al., 1995) and inhibit NK cytotoxicity (Chuang et al., 19941), did not affect actin accumulation or organization, but inhibited LFA-1 reorganization at the IS. At micromolar levels, taxol inhibits the association of microtubule plus end binding proteins ("plus end tracking proteins") such as EB1 (Morrison et al., 1998) and CLIP170 (Perez et al., 1999). Therefore, microtubule dynamic instability and/or the presence of specific microtubule plus end binding

proteins could be required for LFA-1 reorganization at the IS. In this regard, in T cells, the α-tubulin deacetylase HDAC6, translocates to the IS where it regulates α-tubulin deacetylation and LFA-1 organization (Serrador et al., 2004). HDAC6 increases microtubule dynamics instability, which correlates with its interaction with EB1 (Zilberman et al., 2009) and with CLIP170 (Li et al., 2014). Therefore, it would be interesting to investigate if HDAC6 and/or specific microtubule plus end binding proteins are involved in LFA-1 reorganization at the lytic IS in NK cells.

Our results demonstrate that, upon NK cell interaction with susceptible targets, AKAP350 partially translocates from the centrosome to the Golgi apparatus. Therefore, we analyzed if there was a specific role of AKAP350 at the Golgi apparatus. Even though it is well established that the Golgi apparatus translocates to the IS during NK lytic response (Kupfer et al., 1983), to our knowledge, the role of this organelle in the development of NK lytic IS has not been examined so far. We found that AKAP350 delocalization from the Golgi apparatus inhibits LFA-1 reorganization at the IS, underscoring the relevance of AKAP350 location at this organelle for the development of NK lytic IS. Furthermore, interference with the Golgi apparatus function with BFA treatment, inhibited LFA-1 reorganization at the IS inhibiting YTS citolytic activity, which reassures that the Golgi apparatus have regulatory effects on the maturation of the IS. The presence of AKAP350 at the Golgi apparatus has been mainly associated with the role of this organelle in microtubule nucleation (Rivero et al, 2009, Ori-McKenney et al, 2012; Maia et al, 2013, Tonucci et al, 2018). Microtubule nucleation in lymphocytes has been typically attributed to the centrosome, which, in fact, is commonly denoted as MTOC. We found that LFA-1/CD28 activated NK cells nucleate microtubules both at the centrosome and at the Golgi apparatus. In those conditions, the decrease in AKAP350 expression specifically inhibits microtubule nucleation at the

Golgi. Those results are in line with studies that showed that the decrease in AKAP350 expression inhibits microtubule nucleation at the Golgi, without having a significant impact on centrosomal nucleation of microtubules (Larocca et al, 2006; Rivero et al, 2009; Tonucci et al, 2018). Golgi-derived microtubules are particularly stable, which correlates with their enrichment in post-translationally modified tubulin (reviewed in Sanders et al., 2015). In fact, the study that first characterized the Golgi apparatus role as a MTOC showed that Golgi-nucleated microtubules become rapidly acetylated (Chabin-Brion et al., 2001). A recent study in motile T cells showed that AKAP350 participates in microtubule nucleation at the centrosome and at extra-centrosomal nucleation centers (Ong et al., 2018). Although this study did not identify microtubule nucleation at the Golgi, it showed that the decrease in AKAP350 expression led to decreased levels of acetylated α-tubulin. Consistently, we found that either the decrease in AKAP350 expression or its delocalization from the Golgi apparatus elicited a decrease in acetylated α-tubulin levels. Altogether, our results demonstrate that the Golgi apparatus participates in cytolytic IS maturation in NK cells, and strongly suggest that Golgi derived microtubules are involved in this effect. How Golgi-derived microtubules can affect NK cytolytic IS maturation deserves further investigation. In this regard, different studies indicate that those non-radial, highly stable tracks support the directionality of Golgi associated polarized trafficking, (reviewed in Sanders and Kaverina, 2015). In connection with that point, studies performed in T cells show that the Golgi apparatus regulates the two way vesicle trafficking to the IS of signaling proteins that are essential for IS maturation (Carpier et al., 2018). Our future studies will address how this particular set of microtubules modulate Golgi derived trafficking and the relevance of this trafficking for the maturation of the lytic IS in NK cells.

MATERIALS AND METHODS

NK and target cell lines

The immortalized NK cell line YTS [Drexler, and Matsuo. 2000] and the cell line KT86, derived from the MHC class I-negative K562 erythroleukemia cell line stably expressing CD86 [Parry et al, 2003], used as susceptible target cell, were obtained from Dr. Jordan Orange lab (Texas Children's Hospital, Houston, TX, USA). Cells were maintained in RPMI medium 1640 supplemented with 10% FBS, 1% L-glutamine, 1% non-essentials amino acids and 1% streptomycin/ampicillin mixture at 37° C and 5% CO_2 atmosphere.

Reduction of AKAP350 expression

In order to reduce AKAP350 expression in YTS cells, we proceeded as we have described previously [Tonucci et al., 2015]. Constructs were made by annealing and ligating oligonucleotides targeting two specific AKAP350 sequences (shRNA1, 5′-CCCAGCTCACTGCTAATTT-3′; shRNA4, 5′-GCAAGAACTAGAACGAGAA-3′) or a scrambled control into the AgeI and EcoRI cloning sites of pLKO.1-puro vector (details at http://www.addgene.org). These constructs were sequenced and used to co-transfect human embryonic kidney 293 FT cells with Virapower lentiviral packaging mix (Invitrogen, Carlsbad, CA). The next day, transfection complexes were removed, and cells were allowed to produce virus for 24 h. Media containing viruses were collected and used to directly transduce YTS cells overnight. The cells were allowed to recover for 24 h and subjected to puromycin selection (2 μg/ml) for 2 weeks. Silencing was confirmed by western blotting and immunofluorescence analyses.

CFSE-based Cytotoxic assay

In order to determine the lytic capacity of YTS cells, we proceed as described in [Jedema et al. 2004]. KT86 cells were washed with PBS , resuspended at 2 x10^6 cells/mL and labeled with 300 nM CFSE (BD Horizont) for 15 min at 37°C. The reaction was stopped by the addition of an equal volume of fetal bovine serum (FCS), followed by a 2-min incubation at room temperature. CFSE-labeled target cells were washed twice and resuspended in RPMI complete medium. The cell concentration was adjusted to 5 x 10^5 cells/mL, and 100 µL/tube were plated in Eppendorf tubes. YTS cells were added at different effector:target ratios. Tubes were incubated in a humidified atmosphere of 5% CO2 and 37°C for 3 hours. For dead cells staining, propidium iodide (1 µg/mL) was added, and samples were mixed properly and directly analyzed by flow cytometry using a BD FACSAria II flow cytometer. 10000 events were acquired for each sample.

FACS-based conjugation assay

YTS cells were washed with PBS, resuspended to 1 x 10^6 cells/ml and labeled with 1.5 mM Cell TrackerTM Deep Red (Invitrogen) for 20 min at 37° C. The reaction was stopped by the addition of an equal of fetal bovine serum, followed by a 5 min incubation at room temperature. After two washes with PBS, the YTS-labeled cells were resuspended in RPMI complete medium. Target cells were labeled with 300 nM CFSE (BD Horizon) as described above. Cells were combined at an effector to target ratio of 2:1 or 10:1 and incubated at 37º C for different periods, as indicated. The samples were gently vortexed for 3 s and immediately fixed with 2% paraformaldehyde (PFA). Samples were run in triplicates and 50000 events were counted for each replicate. The frequency of double positive events was determined within the CFSE positive population using FlowJo software. The following gating strategy was used: First, cells were gated to exclude debris. Compensation adjustments were made on this population using single-positive cells stained for either Cell TrackerTM Deep Red or CFSE. Gates were set to

differentiate between the double positives, represented in G2, from the single positives and double negatives.

Immunofluorescence

KT86 were labeled with 300 nM CFSE (BD Horizon) as described above. Conjugates between YTS cells and KT86 at a 2:1 ratio were established in suspension for 15 min at 37 ° C and adhered to poly-lysine-coated glass slides (Polyprep; Sigma-Aldrich) for additional 15 min. In experiments evaluating NK cell activation by means of specific activating receptors, poly– l -lysine – coated glass slides were coated with anti-CD28, or ICAM-1 by overnight incubation with 5 µg/mL of antibody in PBS. Slides were washed, and NK cells were incubated on the slide for 30 min at 37 ° C. Non adherent cells were washed and cells adhering to the slide were fixed with 4% PFA at room temperature or methanol at -20° C. Fixed cells were permeabilized and blocked with 0.3%Triton X-100/1% bovine serum albuminin/PBS, pH 7.4, for 10 min. Then, they were incubated for 2 h with mouse monoclonal antibody anti CIP4 (BD transduction-612556), anti-LFA-1 (Biolegend 301202) or anti AKAP350 (Schmidt et al, 2001) and rabbit monoclonal antibody anti γ-tubulin (Sigma-T5192) . The coverslips were washed, incubated for 1 h with the secondary antibodies conjugated to Alexa 488, Alexa 560 or Alexa 633 or with phalloidin-Alexa 568 or phalloidin-Alexa 633 (Molecular probes-A34055, 1:200) for actin staining and with 4′,6-diamidino-2-phenylindole (DAPI) and mounted with ProLong (Invitrogen). Fluorescence was detected using LSM880 confocal with an ObserverZ1 inverted microscope. Serial optical 0.2 µm thick sections were collected in the z-axis. Z-stacks were built, and projections were obtained using ImageJ tools. In preparing the figures, adjustment in brightness and contrast were equally applied to the entire images using Adobe Photoshop software to improve visualization of fluorescence.

Image analysis

Centrosome polarization during IS formation, YTS:KT86 conjugates were stained with anti γ-tubulin and DAPI, for centrosome and nucleus identification. The IS was defined as the cell to cell contact region identified in the images obtained by differential interference microscopy (DIC). The cell perimeter of the YTS cell forming the IS was drawn using the same images. The centrosome region was delimited by setting a threshold on the γ-tubulin channel to define a mask, which was used to automatically outline the centrosomal pixels. The IS, the centrosome, and the cell centroid were determined using the appropriate ImageJ tool and the distances from the cell or the centrosome centroid to the IS centroid were calculated. Alternatively, for analysis of centrosome translocation during specific LFA-1 or CD28 activation, the surface of YTS interaction with the ICAM-1 or anti-CD28 coated slides was considered as the IS site, and the distance was measured at the *(y,z)* plane. At least 30 cells from three independent experiments were analyzed for each condition.

For protein accumulation at the IS, YTS cells conjugated with KT86 cells were analyzed. We used DIC images for IS and cell selections. The IS ROI was defined as the closest area to the cell-cell contact site. We measured fluorescence intensity at YTS IS and total fluorescence intensity of the YTS cell (T). The percentage of protein accumulation was calculated as the ratio IS/T.

Centrosomal localization of CIP4 or AKAP350 was determined in images obtained by confocal microscopy by setting a threshold on γ-tubulin channel to define a mask, which was used to automatically outline the centrosomal voxels, and a threshold on CIP4 or AKAP350 channels to define a mask to automatically outline total voxels for each protein staining. Average and total intensity of fluorescence in the CIP4 or AKAP350 channels

was measured in each region of interest, and the ratio of centrosomal and total cell levels calculated.

Golgi levels of AKAP350 were determined in images obtained by confocal microscopy by setting a threshold on GM130 channel to define a mask, which was used to automatically outline the Golgi voxels. Total intensity of fluorescence in the AKAP350 channel was measured in each region of interest. In addition, total AKAP350 levels were determined in a region delimited by a mask defined using the AKAP350 channel, and the percentage of AKAP350 fluorescence at the Golgi apparatus calculated.

Immunoblotting

Cells were harvested at 400 *g* for 5 min at room temperature and washed with cold PBS. Pelleted cells were lysed in ice-cold lysis buffer (50 mM Tris-HCl [pH 7.5], 100 mM NaCl, 15 mM EDTA and 1% Triton X-100, with protease inhibitors) and subjected to two freeze–thaw cycles. Lysates were centrifuged at 1000 *g* for 5 min at 4° C, and the clear supernatants were conserved. Total protein concentrations were measured according to Lowry *et al*. (1951). Samples were heated for 10 min at 90 °C in sample buffer (20 mM Tris-HCl, pH 8.5, 1% SDS, 400 μM DTT, 10% glycerol). Samples containing equal amounts of proteins were subjected to SDS polyacrylamide gel electrophoresis (6–10% gradient to verify AKAP350 silencing or 10% otherwise). The proteins in the 6% gel were transferred to nitrocellulose membranes (Amersham Pharmacia Biotech), whereas the 10% gel proteins were transferred to polyvinyl difluoride membranes (Perkin Elmer Life Sciences). Blots were blocked with 5% nonfat dry milk in PBS, 0.3% Tween-20 (PBS-Tween). Nitrocellulose blots were then probed with the monoclonal mouse anti-AKAP350 antibody (1:500), and polyvinyl difluoride membranes were probed with mouse monoclonal antibodies anti-α-tubulin (Sigma-T9026, 1:5000) or anti-CIP4. The blots were washed and incubated with the horseradish peroxidase-conjugated

corresponding secondary antibodies, and bands were detected by enhanced chemiluminescence (Pierce, Thermo Scientific). Autoradiographs were obtained by exposing the blots to Kodak XAR film. The bands were quantitated by densitometry using the NIH Image J program.

Preparation of centrosome and microtubule enriched subcellular fractions.

Centrosome-enriched fractions were prepared by centrifugation on a Fycoll cushion, using a method based on Blomberg-Wirschell and Doxsey [1998]. Briefly, cells were treated with Nocodazole (1.65 μM) and Cytochalasin (390 ηM) for 30 min, and washed with PBS. Cells were resuspended and gently sonicated in a lysis buffer containing 1Mm TRIS-HCl [pH 8], 0.5% β-Mercaptoethanol, 0.5% Triton X-100 and protease inhibitors. Components were added to cell lysates to achieve a final concentration of 10 mM PIPES, 1 mM EDTA. In order to eliminate unbroken cells and nuclear fractions, cell extracts were centrifuged at 1,500 *g* for 15 min. The supernatant was filtered through a nylon mesh and loaded on the top of a 20% (w/v) Ficoll cushion in buffer 10 mM PIPES/1 mM EDTA with 0.1% Triton X-100 and tubes were spun at 25,000 g in a swinging bucket rotor. Centrosomes were taken from the top of the Ficoll cushion using a Pasteur pipet, and CIP4 levels at this fraction were analysed by western blot.

Cellular extracts enriched in stable microtubules were prepared based on a non ionic detergent extraction protocol described by Brown et al (1992). A total of $4x10^6$ YTS cells were harvested and added on plastic wells coated with ICAM-1 and CD28 for 30 minutes at 37°C. Cells were rinsed once with PBS and once with PHEM (60 mM Pipes, 25 mM Hepes, 10 mM EGTA, 2 mM MgC12, pH 6.9) and then extracted for 5 min in PHEM containing 0.1% Tritón X-100, 10 μM taxol and a mixture of protease inhibitors. Then, the cells were washed with PHEM without Tritón and scrapped with a 100 μL of sample buffer. The protein-contained sample buffer was collected into eppendorf tubes and

incubated for 10 minutes at 90°C . The proteins associated with microtubules were analyzed by western blot.

YTS cells treatments

In order to assess the role of microtubules on the Immune Synapse formation, YTS cells were harvested and 2.10^{6} cells were treated for 1 hour with nocodazole (17 µM) on ice or for 1 hour with Taxol (10 µM) at room temperature and then allowed to form conjugates with KT86 cells at a 2:1 ratio for 15 min at 37° C. After that, the conjugates were adhered to poly – l -lysine – coated glass slides (Polyprep; Sigma-Aldrich) for 15 min at 37 ° C. Then, the conjugates were with 4% PFA and stained with phalloidin Alexa Fluor 555, antibody anti LFA-1. In order to evaluate the role of Golgi derived microtubules on Immune Synapse formation, YTS cells were treated with Brefeldin A (5 µg/ml) for 30 min at 37 ° C. After Brefeldin A treatment, YTS cells were allowed to form conjugates with KT86 cells at a 2:1 ratio for 15 min at 37° C. Then, the conjugates were adhered to poly – l -lysine – coated glass slides (Polyprep; Sigma-Aldrich) for 15 min at 37 ° C. Then, cells were fixed with PFA 4% and stained with antibody anti GM130 and phalloidin Alexa Fluor 555 or antibody anti LFA-1. An additional group YTS cells without drug treatment was used as control. The conjugates were analyzed by confocal microscopy as described previously.

Ice recovery assay

A total of $2x10^{5}$ YTS cells were placed on poly-l-lysine-coated coverslips coated with ICAM-1 and CD28 and incubated for 30 minutes at 37°C. Then, coverslips were incubated on ice 50 min and allowed to recover at room temperature. For analysis of Golgi and centrosome nucleation of microtubules, cells were recovered for 3 or 7 minutes and immediately treated 45 s with extraction buffer (60 mM PIPES, 25 mM

HEPES, 10 mM EGTA, 2 mM MgCl2, 0.1% Tritón X-100, pH 6.9, supplement with 0.25 nM nocodazole and 0.25 nM paclitaxel). Cells were then fixed with methanol and stained with antibody anti GM130 (#catálogo) and antibody anti α-tubulin (Sigma-T9026).

REFERENCES

Aspenström PA. Cdc42 target protein with homology to the non-kinase domain of FER has a potential role in regulating the actin cytoskeleton. *Curr Biol*. 1997; 7: 479-87

Aspenström P, Richnau N, Johansson AS. The diaphanous-related formin DAAM1 collaborates with the Rho GTPases RhoA and Cdc42, CIP4 and Src in regulating cell morphogenesis and actin dynamics. Exp. Cell Res. 2006; 312:2180-2194.

Banerjee PP, Pandey R, Zheng R, Suhoski MM, Monaco-Shawver L, Orange JS. Cdc42-interacting protein-4 functionally links actin and microtubule networks at the cytolytic NK cell immunological synapse. J Exp Med. 2007; 204:2305-20.

Blomberg-Wirschell, M. & Doxsey, S. J. Rapid isolation of centrosomes. *Methods Enzymol.* **298**, 228–38 (1998).

Brown ACN, Oddos S, Dobbie IM, Alakoskela J-M, Parton RM, et al. (2011) Remodelling of Cortical Actin Where Lytic Granules Dock at Natural Killer Cell Immune Synapses Revealed by Super-Resolution Microscopy. PLoS Biol 9(9): e1001152.

Brown A, Slaughter T, Black MM. Newly Assembled Microtubules Are Concentrated in the Proximal and Distal Regions of Growing Axons. J Cell Biol. 1992; 119: 867-882

Butler B, Cooper JA. Distinct roles for the actin nucleators Arp2/3 and hDia1 during NK-mediated cytotoxicity. Curr Biol 2009; 19: 1886–1896.

Carlin LM, Evans R, Milewicz H, Fernandes L, Matthews DR, Perani M, Levitt J, Keppler MD, Monypenny J, Coolen T, Barber PR, Vojnovic B, Suhling K, Fraternali F, Ameer-Beg S, Parker PJ, Thomas NS, Ng T. A targeted siRNA screen identifies regulators of Cdc42 activity at the natural killer cell immunological synapse Sci Signal. 2011; 4:ra81.

Carpier JM et al. Rab6-dependent retrograde traffic of LAT controls immune synapse formation and T cell activation. J. Exp. Med. (2018) 215, 1245–1265.

Chabin-Brion K, Marceiller J, Perez F, Settegrana C, Drechou A, Durand G, Poüs C . The Golgi complex is a microtubule-organizing organelle. Mol Biol Cell. 2001; 12:2047-60.

Chardin P, McCormick F. Brefeldin A: The Advantage of Being Uncompetitive. Cell. 1999; 97:153-155.

Chen X, Allan DS, Krzewski K, Ge B, Kopcow H, Strominger JL. CD28-stimulated ERK2 phosphorylation is required for polarization of the microtubule organizing center and granules in YTS NK cells. Proc. Natl. Acad. Sci. USA. 2006; 103:10346–10351.

Chuang, L.T.; Lotzová, E.; Heath, J.; Cook, K.R.; Munkarah, A.; Morris, M.; Wharton, J.T. Alteration of lymphocyte microtubule assembly, cytotoxicity, and activation by the anticancer drug taxol. Cancer Res. 1994, 54, 1286–1291.

Derry WB, Wilson L, Jordan MA. Substoichiometric Binding of Taxol Suppresses Microtubule Dynamics. Biochemistry 1995,34, 2203-2211

Drexler, H. G., Y. Matsuo. 2000. Malignant hematopoietic cell lines: in vitro models for the study of natural killer cell leukemia-lymphoma. Leukemia 14: 777-782

El Din El Homasany BS, Volkov Y, Takahashi M, Ono Y, Keryer G, Delouvée A, Looby E, Long A, Kelleher D. 2005. The scaffolding protein CG-NAP/AKAP450 is a

critical integrating component of the LFA-1-induced signaling complex in migratory T cells. J Immunol. 175:7811-8.

Florian S, Mitchison TJ. Anti-Microtubule Drugs. Methods Mol Biol. 2016;1413:403-21. doi: 10.1007/978-1-4939-3542-0_25.

Fong A, Durkin A, and Lee H. Int. The Potential of Combining Tubulin-Targeting Anticancer Therapeutics and Immune Therapy J. Mol. Sci. 2019, 20, 586; doi:10.3390/ijms20030586.

Grimaldi AD, Fomicheva M, Kaverina I. Ice recovery assay for detection of Golgi-derived microtubules. Methods Cell Biol. 2013; 118:401-15.

Hurtado L, Caballero C, Gavilan MP, Cardenas J, Bornens M, Rios RM. Disconnecting the Golgi ribbon from the centrosome prevents directional cell migration and ciliogenesis. J Cell Biol. 2011 May 30;193(5):917-33.

Jedema, Inge, et al. "New CFSE-based assay to determine susceptibility to lysis by cytotoxic T cells of leukemic precursor cells within a heterogeneous target cell population." *Blood* 103.7 (2004): 2677-2682.

Katz P, Zaytoun AM and Lee J H Jr. Mechanisms of human cell-mediated cytotoxicity. III. Dependence of natural killing on microtubule and microfilament integrity. J Immunol 1982, 129: 2816-2825.

Kupfer A, Dennert G, Singer SJ. Polarization of the Golgi apparatus and the microtubule-organizing center within cloned natural killer cells bound to their targets. Proc Natl Acad Sci USA 1983; 80: 7224–7228.

Kim HS, Takahashi M, Matsuo K, Ono Y Recruitment of CG-NAP to the Golgi apparatus through interaction with dynein-dynactin complex. Genes Cells. 2007; 12:421-34.

Kolobova E, Roland JT, Lapierre LA, Williams JA, Mason TA, Goldenring JR. The C-terminal region of A-kinase anchor protein 350 (AKAP350A) enables formation of microtubule-nucleation centers and interacts with pericentriolar proteins. J Biol Chem. 2017; 292: 20394–20409. doi: 10.1074/jbc.M117.806018

Lagrue K, Carisey A, Oszmiana A, Kennedy PR, Williamson DJ, Cartwright A, Barthen C, Davis DM.. The central role of the cytoskeleton in mechanisms and functions of the NK cell immune synapse. Immunological Reviews 2013. Vol. 256: 203–221

Larocca MC, Jin M, Goldenring JR. AKAP350 modulates microtubule dynamics. Eur J Cell Biol. 2006; 85:611-9. doi: 10.1016/j.ejcb.2005.10.008.

Larocca MC, Shanks RA, Tian L, Nelson DL, Stewart DM, Goldenring JR. AKAP350 interaction with cdc42 interacting protein 4 at the Golgi apparatus. Mol Biol Cell. 2004; 15:2771-81.

Leibfried A, Fricke R, Morgan MJ, Bogdan S, Bellaiche Y. Drosophila Cip4 and WASp define a branch of the Cdc42-Par6-aPKC pathway regulating E-cadherin endocytosis. Curr Biol. 2008; 18:1639-48.

Li D, Sun X, Zhang L, Yan B, Xie S, Liu R, Liu M, Zhou J. Histone deacetylase 6 and cytoplasmic linker protein 170 function together to regulate the motility of pancreatic cancer cells. Protein Cell. 2014; 5: 214–223. doi: 10.1007/s13238-013-0010-3

Maia A. R., Zhu X., Miller P., Gu G., Maiato H., Kaverina I. (2013). Modulation of Golgi-associated microtubule nucleation throughout the cell cycle. Cytoskeleton 70, 32–43. 10.1002/cm.21079.

Mace EM, Dongre P, Hsu H-T, Sinha P, James AM, Mann SS, Forbes LR, Watkin LB, Orange JS. Cell biological steps and checkpoints in accessing NK cell cytotoxicity. Immunol Cell Biol. 2014; 92: 245–255.

Mattaloni SM, Kolobova E, Favre C, Marinelli RA, Goldenring JR, Larocca MC. AKAP350 Is involved in the development of apical "canalicular" structures in hepatic cells HepG2. J Cell Physiol. 2012; 227:160-71. doi: 10.1002/jcp.22713.

Morrison MM, Wardleworth BN, Askham JM, Markham AF, Meredith DM. EB1, a Protein Which Interacts With the APC Tumour Suppressor, Is Associated With the Microtubule Cytoskeleton Throughout the Cell Cycle. Oncogene 1998;17(:3471-7. doi: 10.1038/sj.onc.1202247.

Murugesan S, Hong J, Yi J, Li D, Beach JR, Shao L, Meinhardt J, Madison G, Wu X, Betzig E, Hammer JA. Formin-generated actomyosin arcs propel T cell receptor microcluster movement at the immune synapse. J Cell Biol. 2016; 215:383-399.

Ong ST, Chalasani MLS, Fazil MHUT, Prasannan P, Kizhakeyil A, Wright GD, Kelleher D, Verma NK. Centrosome- and Golgi-Localized Protein Kinase N-Associated Protein Serves As a Docking Platform for Protein Kinase A Signaling and Microtubule Nucleation in Migrating T-Cells. Front Immunol. 2018; 9:397. doi: 10.3389/fimmu.2018.00397

Orange JS, et al. Wiskott-Aldrich syndrome protein is required for NK cell cytotoxicity and colocalizes with actin to NK cell-activating immunologic synapses. Proc Natl Acad Sci USA 2002;99:11351–11356.

Orange JS, Harris KE, Andzelm MM, Valter MM, Geha RS, Strominger JL. The Mature Activating Natural Killer Cell Immunologic Synapse Is Formed in Distinct Stages. Proc Natl Acad Sci USA. 2003; 100:14151-6. doi: 10.1073/pnas.1835830100.

Ori-McKenney, K. M., Jan, L. Y., & Jan, Y.-N. (2012). Golgi outposts shape dendrite morphology by functioning as sites of acentrosomal microtubule nucleation in neurons. Neuron, 76, 921– 930.

Parry, Richard V., et al. CD28 and inducible costimulatory protein Src homology 2 binding domains show distinct regulation of phosphatidylinositol 3-kinase, Bcl-xL, and IL-2 expression in primary human CD4 T lymphocytes. The Journal of immunology, 2003, vol. 171, no 1, p. 166-174.

Perez, F., G.S. Diamantopoulos, R. Stalder, and T.E. Kreis. 1999. CLIP-170 highlights growing microtubule ends in vivo. Cell. 96:517–527.

Rak GD, Mace EM, Banerjee PP, Svitkina T, Orange JS. 2011. Natural killer cell lytic granule secretion occurs through a pervasive actin network at the immune synapse. PLoS Biol 9:e1001151. doi: 10.1371/journal.pbio.1001151.

Rivero S, Cardenas J, Bornens M, Rios RM. Microtubule nucleation at the cis-side of the Golgi apparatus requires AKAP450 and GM130. EMBO J. 2009, 281016-28.

Roberts-Galbraith RH & Gould KL. Setting the F-BAR: functions and regulation of the F-BAR protein family. *Cell Cycle* 2010; 9:4091-4097.

Robles-Valero J, Martín-Cófreces NB, Lamana A, Macdonald S, Volkov Y, Sánchez-Madrid F. (2010) Integrin and CD3/TCR activation are regulated by the scaffold protein AKAP450. Blood. 115:4174-84

Sanders AA, Kaverina I. Nucleation and dynamics of Golgi-derived microtubules. Front Neurosci. 2015;9:431. doi: 10.3389/fnins.2015.00431

Schmidt PH, Dransfield DT, Claudio JO, Hawley RG, Trotter KW, Milgram SL,et al. AKAP350, a multiply spliced protein kinase A-anchoring protein associated with centrosomes. J Biol Chem. 1999; 274:3055-66.

Serrador JM, Cabrero JR, Sancho D, Mittelbrunn, M, Urzainqui A, Sánchez-Madrid F, 2004 HDAC6 Deacetylase Activity Links the Tubulin Cytoskeleton with Immune Synapse Organization. Immunity, 20, 417–428.

Sillibourne JE, Milne DM, Takahashi M, Ono Y, Meek DW. Centrosomal anchoring of the protein kinase CK1delta mediated by attachment to the large, coiled-coil scaffolding protein CG-NAP/AKAP450. J Mol Biol. (2002) 322:785–97. 10.1016/S0022-2836(02)00857-4.

Takahashi M, Yamagiwa A, Nishimura T, Mukai H, Ono Y. Centrosomal Proteins CG-NAP and Kendrin Provide Microtubule Nucleation Sites by Anchoring γ-Tubulin Ring Complex. Mol Biol Cell. 2002; 13: 3235–3245. doi: 10.1091/mbc.E02-02-0112

Tian L, Nelson DL, Stewart, DM. Cdc42-interacting protein 4 mediates binding of the Wiskott-Aldrich syndrome protein to microtubules. *J. Biol. Chem*. 2000; 275:7854-7861.

Tonucci FM, Almada E, Borini-Etichetti C, Pariani A, Hidalgo F, Rico MJ, Girardini J, Favre C, Goldenring JR, Menacho-Marquez M, Larocca MC. Identification of a CIP4 PKA phosphorylation site involved in the regulation of cancer cell invasiveness and metastasis. Cancer Lett. 2019; 461:65-77. doi: 10.1016/j.canlet.2019.07.006.

Tonucci FM, Ferretti A, Almada E, Cribb P, Vena R, Hidalgo F, Favre C, Tyska MJ, Kaverina I, Larocca MC. Microtubules regulate brush border formation. J Cell Physiol. 2018; 233:1468-1480. doi: 10.1002/jcp.26033.

Tonucci FM, Hidalgo F, Ferretti A, Almada E, Favre C, Goldenring JR, Kaverina I, Kierbel A, Larocca MC. Centrosomal AKAP350 and CIP4 act in concert to define the polarized localization of the centrosome and Golgi in migratory cells. J Cell Sci. 2015; 128:3277-89. doi: 10.1242/jcs.170878.

Tsujita K, Suetsugu S, Sasaki N, Furutani M, Oikawa T, Takenawa T. Coordination between the actin cytoskeleton and membrane deformation by a novel membrane tubulation domain of PCH proteins is involved in endocytosis. J. Cell Biol. 2006; 172:269-279.

Zilberman, Y., Ballestrem, C., Carramusa, L., Mazitschek, R., Khochbin, S., and Bershadsky, A. Regulation of microtubule dynamics by inhibition of the tubulin deacetylase HDAC6 J Cell Sci 2009; 122, 3531–3541.

FIGURE LEGENDS

Figure 1. AKAP350 localization in YTS cells. Isolated YTS cells or YTS:KT86 conjugates were stained and analyzed by confocal microscopy as described in Materials and Methods. A,B) Merge images show YTS cells (upper row) or YTS:KT86 conjugates (lower row) staining for AKAP350 (red) and γ-tubulin (A) or GM130 (B) (green). Asterisk denotes YTS cells in YTS:KT86 conjugates. C,D) Bars represent the mean fraction of AKAP350 fluorescence present at centrosomes (C) or at the Golgi apparatus (D) in isolated or conjugated YTS cells, expressed as percentage of total AKAP350-fluorescence, representative of three independent experiments. At least 20 cells were analyzed for each experiment. Error bars represent SEM. *$p < 0.05$. Scale bars, 5 μm.

Figure 2. Reduction of AKAP350 expression levels diminishes YTS cells' cytotoxicity. Two different specific shRNAs (shRNA1 and shRNA4) were used to generate YTS cells with decreased AKAP350 expression (AKAP350KD1 and AKAP350KD2, respectively), as described in Materials and methods. A) Western blot analysis of AKAP350 expression in control, AKAP350KD1 and AKAP350KD2 YTS cells. CIP4 was used as loading control. B,C) KT86 cells were stained with CFSE and mixed with YTS cells at 2:1 (B) or 10:1 (C) effector: target ratios. After the incubation period, cells

were stained with PI and analyzed by flow cytometry. YTS cytotoxic activity was estimated as the fraction of total CFSE positive events that were also positive for PI. Bars chart represents the mean percentage of double positive events for control, AKAP350KD1 and AKAP350KD2 cells, representative of three independent experiments. Error bars represent SEM. *$p < 0.05$.

Figure 3. AKAP350 is required for centrosome polarization during YTS cells activation. A) Control and AKAP350KD YTS cells were incubated with CFSE labeled KT86 cells at a 2:1 ratio. Cell conjugates were fixed, stained and analyzed by confocal microscopy. Merge images show staining for AKAP350 (red), γ-tubulin (gray) and DAPI (blue), and CFSE labeled target cells (green). White arrows indicate the position of γ-tubulin-labeled centrosomes in YTS cells. Bars represent the mean distance from the centrosome to the IS, representative of five independent experiments. B,C) Control and AKAP350KD YTS cells were activated using coverslips coated with the LFA-1 activating ligand ICAM-1 (B) or an activating anti-CD28 antibody (C). Activated cells were fixed, stained and analyzed by confocal microscopy. Merge images show γ-tubulin (green) and DAPI (blue) staining. White arrow indicates the position of γ-tubulin-defined centrosomes. White dashed lines denote the cell surface in contact with the coverslip. Bars represent the mean distance from the centrosomes to the cell-coverslip contact surface, representative of three independent experiments. At least 30 conjugates (A) or cells (B,C) were analyzed for each experiment. Error bars represent SEM. Scale bars, 5 μm. *$p<0.05$.

Figure 4. Reduction of AKAP350 expression levels alters CIP4 localization in YTS cells. A) Merge images show staining for CIP4 (red) and γ-tubulin (green) in control and AKAP350KD YTS cells. White arrows mark γ-tubulin defined centrosomes. Bars represent the mean fraction of CIP4 associated fluorescence located at the centrosome,

expressed as percentage of total cell fluorescence in the CIP4 channel, representative of three independent experiments. At least 30 conjugates were analyzed for each experiment. Error bars represent SEM. B) Centrosomes enriched subcellular fractions were prepared by differential centrifugation of control or AKAP350KD cell lysates as described in Materials and Methods. Total cells lysates and centrosomal fractions were analyzed for CIP4 expression by western blot. Bars represent the mean fraction of CIP4 recovered at centrosome-fractions, expressed as percentage of total CIP4 recovery in cell lysates of three independent experiments. C) CIP4 localization during establishment of the IS was analyzed in control and AKAP350KD YTS cells conjugated to KT86 cells at a 2:1 ratio. Merge images show conjugates staining for CIP4 (red) and γ-tubulin (green). White arrows indicate the position of γ-tubulin-defined centrosomes. Bars represent the mean fraction of CIP4 fluorescence located at the centrosome or at the IS, expressed as percentage of total cell fluorescence for the CIP4 channel, representative of three independent experiments. At least 30 conjugates were analyzed for each experiment. Error bars represent SEM. D) Control or AKAP350KD cells were incubated in plates coated with the activating anti-CD28 antibody and ICAM-1. Fractions of stabilized microtubules were obtained with non-ionic detergent extraction as described in Material and methods. CIP4 and α-tubulin recovery in total cell lysates and microtubule-fractions were analyzed by western blot. Bars represent the mean fraction of CIP4 or α-tubulin recovered at microtubule-fractions, expressed as percentage of total yield in cell lysates, and the mean fraction of CIP4 recovered at the microtubule fraction related to α-tubulin recovery for three independent experiments. Scale bars, 5 μm. *$p < 0.05$

Figure 5. Reduction of AKAP350 expression levels results in defective actin and LFA-1 organization at the IS. A) Control and AKAP350KD YTS cells were incubated with

CFSE labeled KT86 cells at a 2:1 ratio. Merge images show YTS:KT86 conjugates staining for actin (red), LFA-1 (cyan) and DAPI (blue). Individual actin and LFA-1 channels are shown in pseudocolor. Bars represent the mean fraction of actin or LFA-1 fluorescence located at the IS, expressed as percentage of total cell fluorescence for each channel, for three independent experiments. At least 30 conjugates were analyzed for each experiment. Error bars represent SEM. B, C) Control and AKAP350KD YTS cells were activated using coverslips coated with ICAM-1 (B) or with the activating anti-CD28 antibody (C). Merge images show actin (red), LFA-1 (green) and DAPI (blue) staining. Individual actin and LFA-1channels are shown in pseudocolor. White dashed lines indicate the cell surface in contact with the coverslip. Bars represent the mean fraction of actin or LFA-1 fluorescence located at the cell surface in contact with the ICAM-1 (B) or anti-CD28 (C) coated coverslip, expressed as percentage of total cell fluorescence for each channel representative of three independent experiments. At least 30 conjugates were analyzed for each experiment. Error bars represent SEM. D) Control and AKAP350KD YTS cells were incubated with CFSE labeled KT86 cells. Images show the X-Z projection of the IS region corresponding to control and AKAP50KD YTS cells. Merge images show LFA-1 (green) and actin (red) staining. Individual LFA-1 and actin channels are shown in pseudocolor. Dashed lines denote the radius of the IS where LFA-1 and actin intensity of fluorescence were quantified. Charts represent the profile of intensity of fluorescence quantified for each channel, representative of at least ten IS analyzed in three independent experiments. Scale bars, 5 μm. *$p<0.05$.

Figure 6. Microtubule dynamics is required for LFA-1 organization at the IS. Control YTS cells or YTS cells treated with nocodazole or taxol (see Materials and methods) were mixed with KT86 cells at a 2:1 ratio. Images show *x,y* planes (first and third

columns) or *x,z* projections (second and fourth columns) of the IS region corresponding to control and nocodazole or taxol treated YTS cells. Merge images show cell conjugates staining for actin (red) and LFA-1 (green). LFA-1 channel is shown in pseudocolor. Dashed lines denote the radius of the IS where LFA-1 intensity of fluorescence was quantified. Charts represent the profile of intensity of fluorescence quantified for the LFA-1 channel, representative of at least ten IS analyzed in three independent experiments. Bars represent the mean fraction of LFA-1 fluorescence located at the IS, expressed as percentage of total cell fluorescence, representative of three independent experiments. At least 30 conjugates were analyzed for each experiment. Scale bars, 5 μm. Error bars represent SEM. *$p<0.05$.

Figure 7. AKAP350 is essential for microtubules nucleation at the Golgi apparatus in activated YTS cells. Control cells or AKAP350KD YTS cells were activated using ICAM-1 and the activating anti-CD28 antibody for 30 minutes and then subjected to ice recovery assays. Merge images show staining for GM130, as a Golgi marker, in red and for α-tubulin in green. Bar charts represent the mean number of microtubules derived from the centrosome or from the Golgi apparatus and the mean fraction of α-tubulin fluorescence associated to each organelle, expressed as percentage of total cell fluorescence for the α-tubulin channel, representative of three independent experiments. At least 10 cells were analyzed for each experiment. Error bars represent SEM. Scale bars, 5 μm. *$p<0.05$

Figure 8. AKAP350 localization at the Golgi apparatus is required for IS maturation. A-C) YTS cells were treated with brefeldin A (BFA) as described in Material and methods. A) KT86 cells were stained with CFSE and mixed with YTS cells at a 2:1 effector: target ratio. After the incubation period, cells were stained with PI and analyzed by flow cytometry. YTS cytotoxic activity was estimated as the fraction of

total CFSE positive events that were also positive for PI. Bars chart represents the mean percentage of double positive events for control and BFA treated cells for three independent experiments. B) Control and BFA treated YTS cells were incubated with KT86 cells. Merge images show staining for LFA-1 (red) and GM130 (gray). LFA-1 channel is shown in pseudocolor. Bars represent the mean fraction of LFA-1 fluorescence located at the IS, expressed as percentage of total cell fluorescence for the LFA-1 channel. More than 30 conjugates were analyzed. Error bars represent SEM. C) Images show the X-Z projection of the IS region corresponding to control and BFA treated YTS cells. Dashed lines denote the radius of the IS where LFA-1 intensity of fluorescence was quantified. Charts represent the profile of intensity of fluorescence, representative of at least ten IS analyzed. D,E) YTS cells with AKAP350 delocalization from the Golgi apparatus by expression of the AKAP350 Golgi binding domain (AKAP350GBD) were prepared as described in Materials and methods. Control and AKAP350GBD YTS cells were incubated with KT86 cells. D) Merge images show YTS:KT86 conjugates staining for actin (red) and LFA-1 (green). Individual actin and LFA-1 channels are shown in pseudocolor. Bars represent the mean fraction of LFA-1 fluorescence located at the IS, expressed as percentage of total cell fluorescence. More than 30 conjugates from 3 different experiments were analyzed. Error bars represent the SEM. E) Images show the X-Z projection of the IS region corresponding to control and AKAP350GBD YTS cells. Dashed lines denote the radius of the IS where LFA-1 intensity of fluorescence was quantified. Charts represent the profile of intensity of fluorescence, representative of at least ten IS. Scale bars, 5 μm. *$p<0.05$.

Figure 1

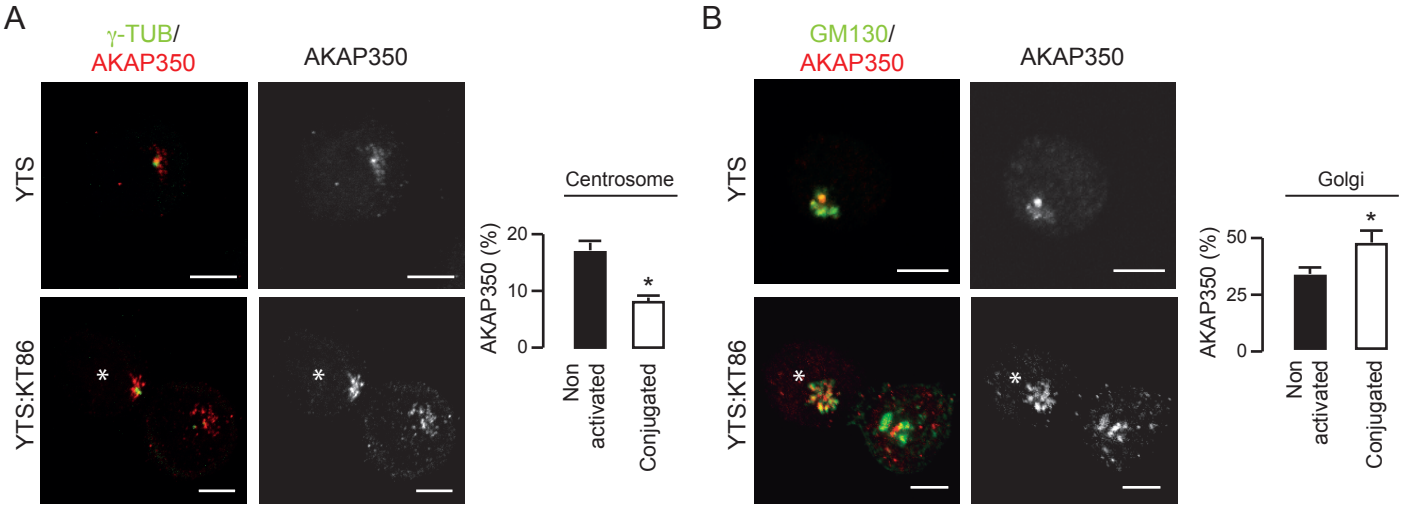
A
γ-TUB/
AKAP350
AKAP350
YTS
YTS:KT86
Centrosome
AKAP350 (%)
20
10
0
Non activated
Conjugated
B
GM130/
AKAP350
AKAP350
YTS
YTS:KT86
Golgi
AKAP350 (%)
50
25
0
Non activated
Conjugated

Figure 2

A

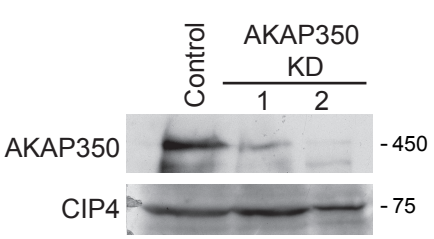
Control
AKAP350 KD
1
2
AKAP350
CIP4
- 450
- 75

B

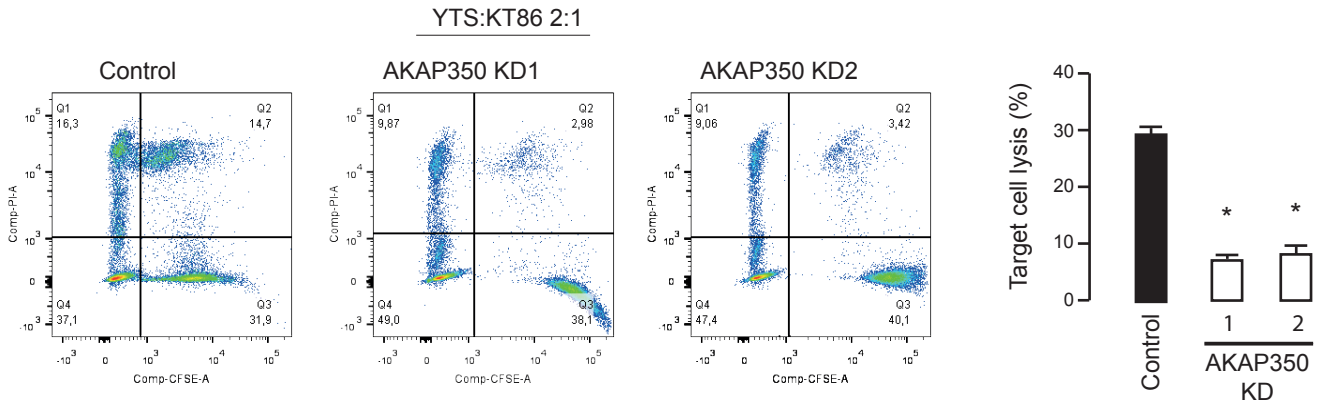
YTS:KT86 2:1
Control
AKAP350 KD1
AKAP350 KD2
Q1 16,3
Q2 14,7
Q4 37,1
Q3 31,9
Q1 9,87
Q2 2,98
Q4 49,0
Q3 38,1
Q1 9,06
Q2 3,42
Q4 47,4
Q3 40,1
Comp-PI-A
Comp-CFSE-A
Target cell lysis (%)
40
30
20
10
0
*
*
Control
1
2
AKAP350 KD

C

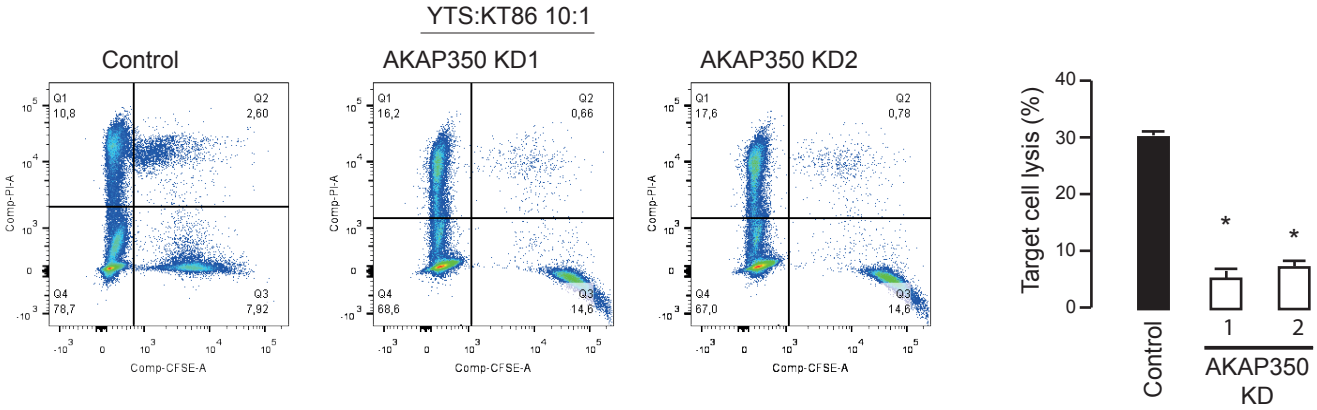
YTS:KT86 10:1
Control
AKAP350 KD1
AKAP350 KD2
Q1 10,8
Q2 2,60
Q4 78,7
Q3 7,92
Q1 16,2
Q2 0,66
Q4 68,6
Q3 14,6
Q1 17,6
Q2 0,78
Q4 67,0
Q3 14,6
Comp-PI-A
Comp-CFSE-A
Target cell lysis (%)
40
30
20
10
0
*
*
Control
1
2
AKAP350 KD

Figure 3

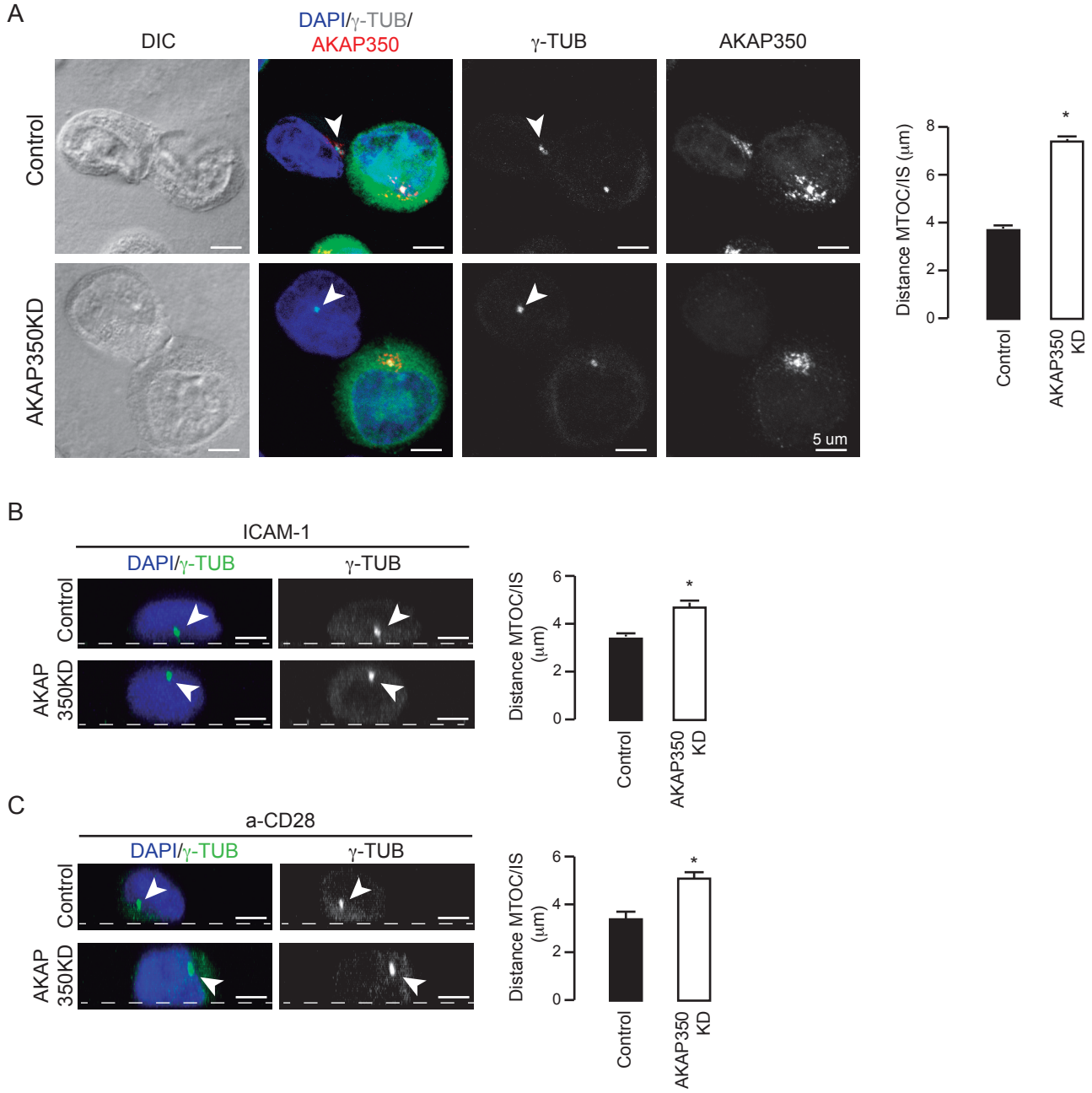
A
DIC
DAPI/γ-TUB/
AKAP350
γ-TUB
AKAP350
Control
AKAP350KD
5 um
Distance MTOC/IS (μm)
0
2
4
6
8
*
Control
AKAP350
KD
B
ICAM-1
DAPI/γ-TUB
γ-TUB
Control
AKAP
350KD
Distance MTOC/IS
(μm)
0
2
4
6
*
Control
AKAP350
KD
C
a-CD28
DAPI/γ-TUB
γ-TUB
Control
AKAP
350KD
Distance MTOC/IS
(μm)
0
2
4
6
*
Control
AKAP350
KD

Figure 4

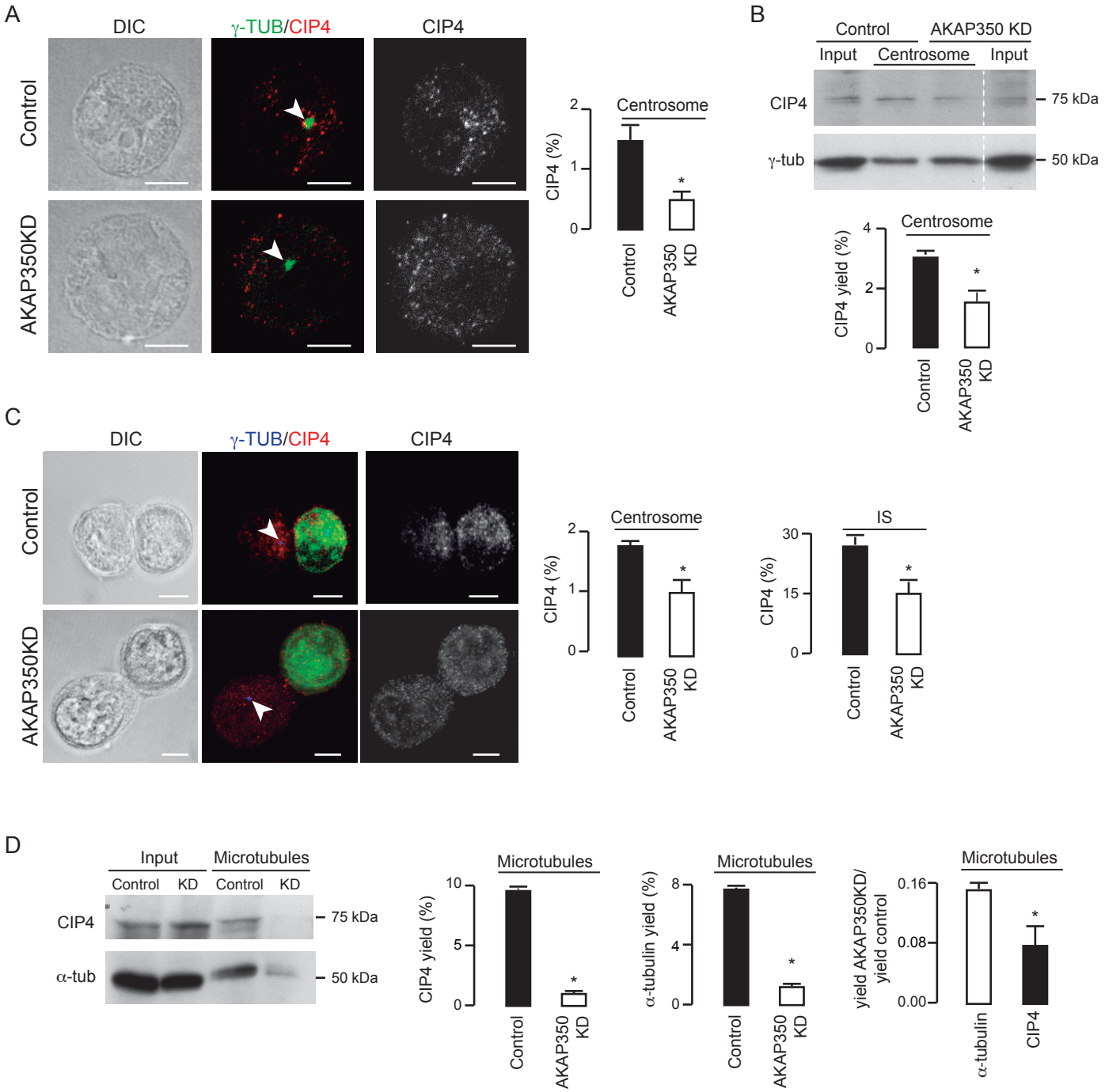
A
DIC
γ-TUB/CIP4
CIP4
Control
AKAP350KD
CIP4 (%)
Centrosome
Control
AKAP350 KD
B
Control
AKAP350 KD
Input
Centrosome
Input
CIP4
γ-tub
75 kDa
50 kDa
CIP4 yield (%)
Centrosome
Control
AKAP350 KD
C
DIC
γ-TUB/CIP4
CIP4
Control
AKAP350KD
CIP4 (%)
Centrosome
IS
Control
AKAP350 KD
D
Input
Microtubules
Control
KD
Control
KD
CIP4
α-tub
75 kDa
50 kDa
CIP4 yield (%)
Microtubules
Control
AKAP350 KD
α-tubulin yield (%)
Microtubules
Control
AKAP350 KD
yield AKAP350KD/ yield control
Microtubules
α-tubulin
CIP4

Figure 5

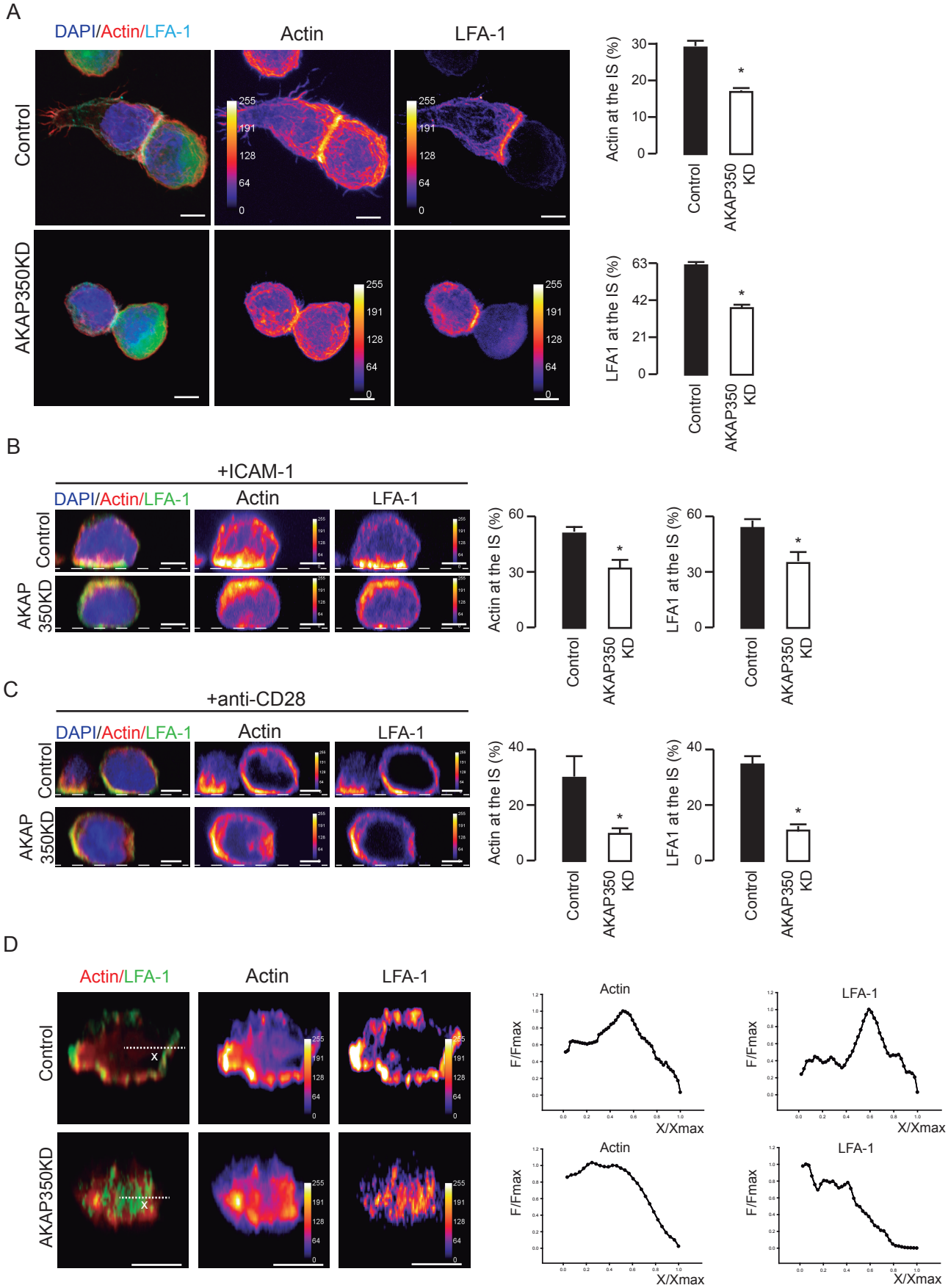
A
DAPI/Actin/LFA-1
Actin
LFA-1
Control
AKAP350KD
255
191
128
64
0
Actin at the IS (%)
LFA1 at the IS (%)
Control
AKAP350 KD
B
+ICAM-1
C
+anti-CD28
AKAP 350KD
D
Actin/LFA-1
F/Fmax
X/Xmax

Figure 6

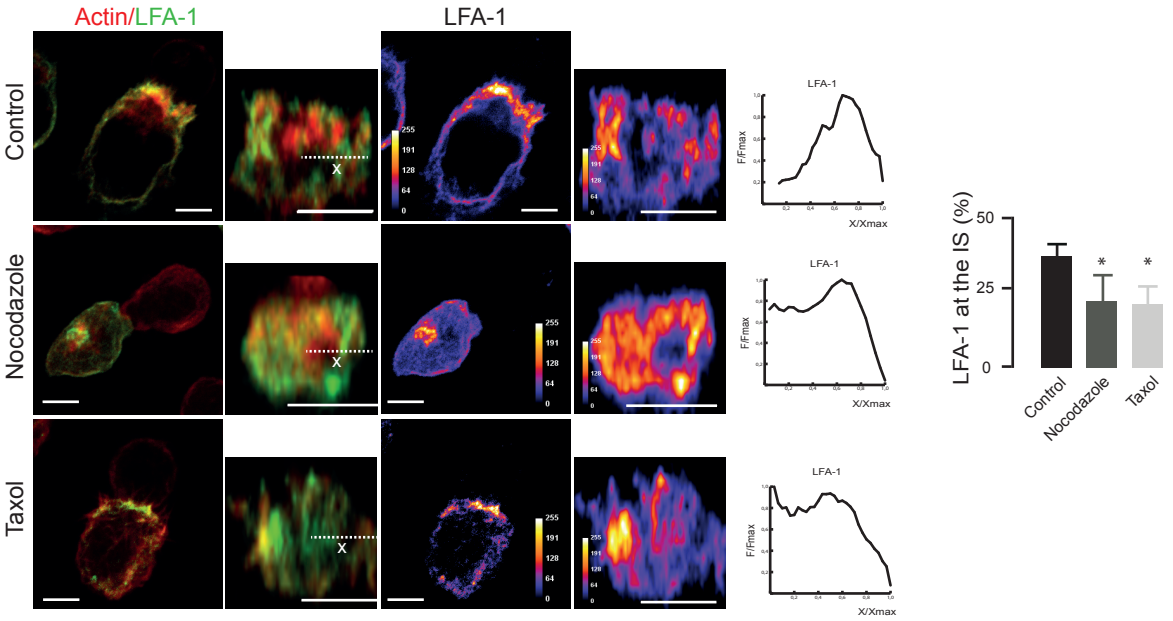
Actin/LFA-1
LFA-1
Control
Nocodazole
Taxol
X
255
191
128
64
0
LFA-1
F/Fmax
X/Xmax
LFA-1 at the IS (%)
50
25
0
*
*
Control
Nocodazole
Taxol

Figure 7

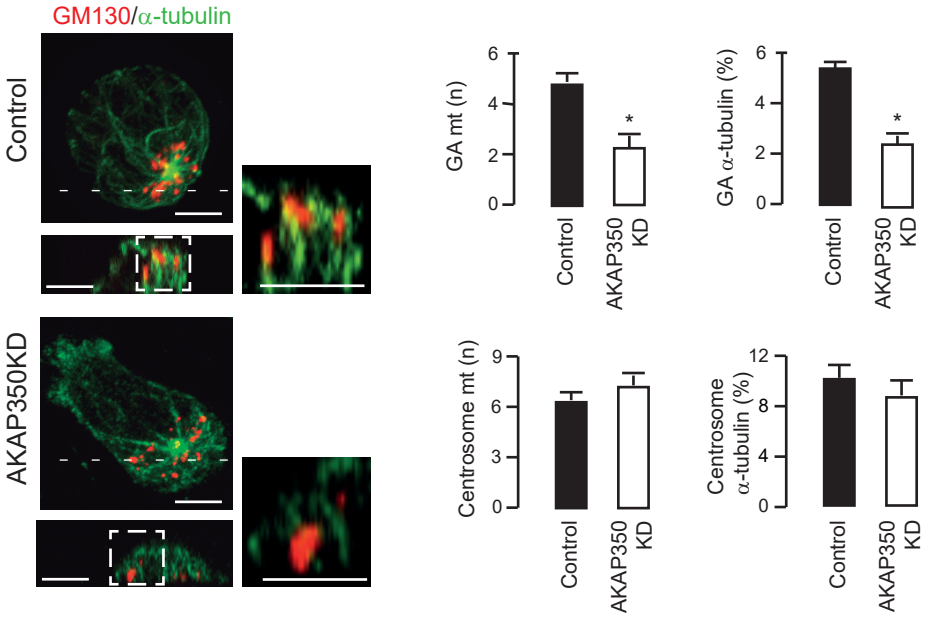
GM130/α-tubulin
Control
AKAP350KD
GA mt (n)
GA α-tubulin (%)
Centrosome mt (n)
Centrosome α-tubulin (%)
Control
AKAP350 KD
*

Figure 8

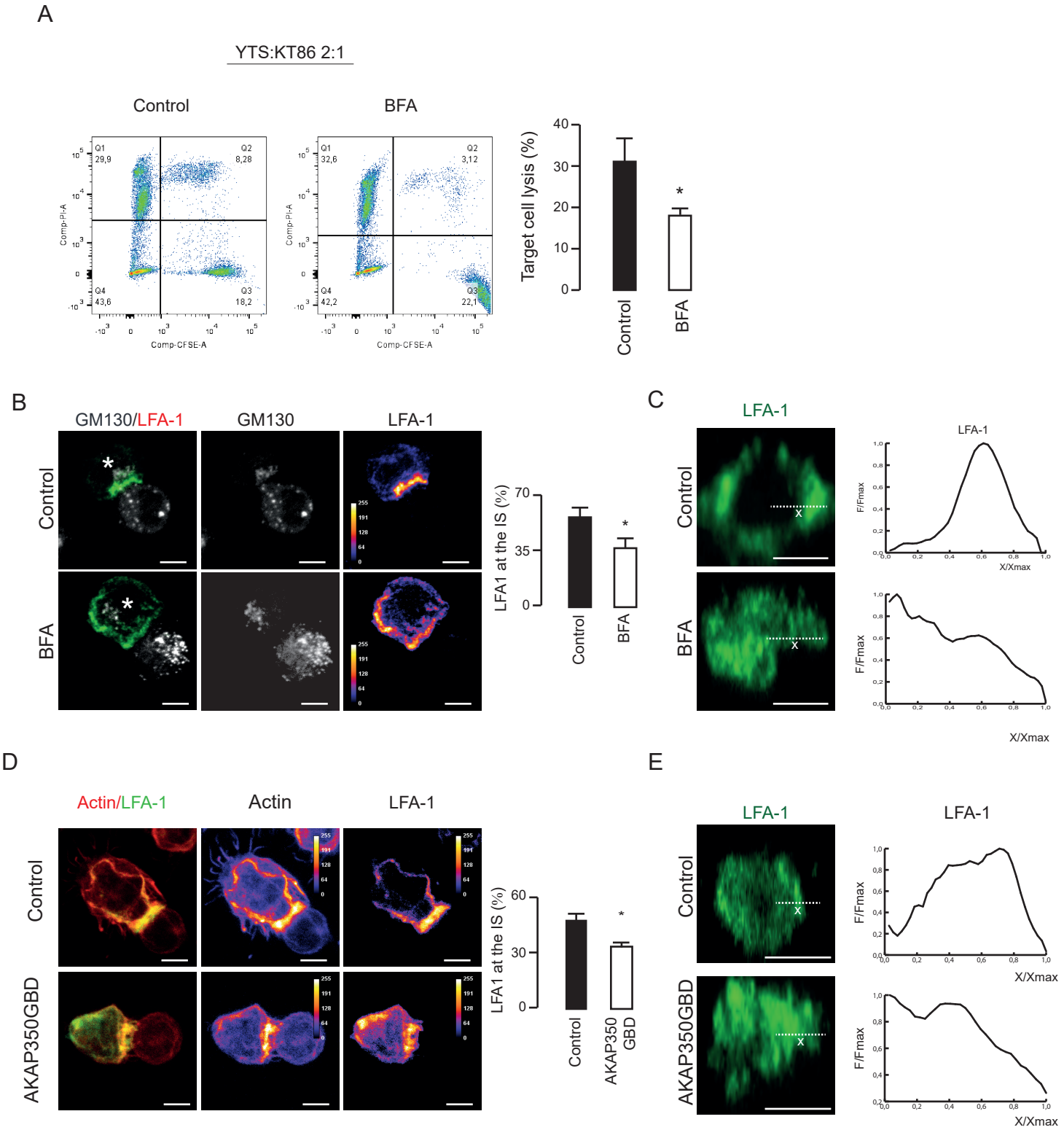
A
YTS:KT86 2:1
Control
BFA
Q1 29,9
Q2 8,28
Q4 43,6
Q3 18,2
Q1 32,6
Q2 3,12
Q4 42,2
Q3 22,1
Comp-PI-A
Comp-CFSE-A
Target cell lysis (%)
40
30
20
10
0
*
Control
BFA
B
GM130/LFA-1
GM130
LFA-1
Control
BFA
*
255
191
128
64
0
LFA1 at the IS (%)
70
35
0
*
Control
BFA
C
LFA-1
Control
BFA
x
F/Fmax
X/Xmax
D
Actin/LFA-1
Actin
LFA-1
Control
AKAP350GBD
LFA1 at the IS (%)
60
30
0
*
Control
AKAP350 GBD
E
LFA-1
LFA-1
Control
AKAP350GBD
x
F/Fmax
X/Xmax